PHYSICS AND CHEMISTRY OF SOLID STATE
V. 26, No. 4 (2025) pp. 802-807
Section: Physics

DOI: 10.15330/pcss.26.4.802-807

Vasyl Stefanyk Carpathian National University

ФІЗИКА І ХІМІЯ ТВЕРДОГО ТІЛА
Т. 26, № 4 (2025) С. 802-807
Фізико-математичні науки

PACS: 81.65.Cf, 72.40.+w, 42.79.Hp, 78.40.Fy, 84.40.-x

ISSN 1729-4428 (Print)
ISSN 2309-8589 (Online)

O. Balaban[1], R. Bukliv[1], A. Danylov[1], B. Venhryn[1], D. Vynnyk[1], V. Haiduchok[2], A. Andrushchak[1]

Effect of Surface Treatment of Single-Crystalline Ge on Its Photoconductivity and Photomodulation of Radiation with frequency of 0.13 THz

[1]*Lviv Polytechnic National University, Lviv, Ukraine, bohdan.y.venhryn@lpnu.ua*
[2]*«Electron-Carat» Scientific-Research Company, Ukraine*

The influence of mechanical processing as well as ion and chemical surface etching of single-crystal germanium on its photoconductivity and photomodulation properties in the terahertz spectral region was investigated. Relative changes in the conductivity of the material under laser illumination at a wavelength of 660 nm and various irradiation powers were determined. A setup was developed for studying the photomodulation properties of germanium at a frequency of 0.13 THz, and a pronounced increase in the absorption of terahertz radiation was revealed even at low illumination powers.

Keywords: Semiconductors, Single-crystal Germanium, Chemical surface etching, Photoconductivity, Terahertz radiation, Photomodulation.

Received 28 May 2025; Accepted 29 October 2025.

Introduction

The rapid development and application of terahertz (THz) technologies [1] have intensified research into methods for controlling and manipulating THz radiation, including its modulation, scanning, and related techniques. THz beam polarization, steering, focusing, and resonator fabrication are key enabling technologies in THz communication and THz coded aperture imaging. Comprehensive reviews of methods for modulating THz and sub-THz radiation at frequencies above 100 GHz, including all-optical, electronic, and thermal modulators, are provided in [2-5]. Among these, all-optical modulators of THz radiation have attracted significant attention due to their relative simplicity, the ability to control THz signals without converting them into electrical form, high data transmission rates, broad signal bandwidths, and low power consumption [6–8]. In such systems, modulation is achieved via an optical source due to the change of the photoconductivity of a modulating material [9, 10]. Semiconductors remain promising candidates for THz modulator fabrication. When light with photon energy exceeding the semiconductor bandgap irradiates the material, non-equilibrium charge carriers are generated, resulting in a change in its photoconductivity. The density of these photoinduced non-equilibrium carriers depends on the intensity of the incident optical radiation. The transmission of THz waves through a photoexcited semiconductor plate is calculated according to the Fresnel formulas and is determined by the wave's angle of incidence, the complex refractive index n, and the material's thickness. It is obvious that the complex refractive index of illuminated semiconductors changes, and, consequently, the transmission of THz waves through these materials changes. The modulation performance is limited by several factors, including operating conditions and the properties of the materials used. One of the promising materials used for THz photomodulation is crystalline Germanium [11, 12]. The high concentration of photogenerated charge carriers and the high modulation depth in Ge samples compared to Si and GaAs are the result of the larger optical absorption coefficient at the

photoexcitation wavelength, higher carrier diffusion coefficient, and the longer carrier lifetime. Although the effects of parameters such as sample thickness and area, illumination power density, and frequency range on photomodulation depth have been explored theoretically [11], experimental data on Ge's response to light illumination, especially considering the surface effects caused by Ge surface treatment, remain limited. Since the surface condition of crystalline Ge plays a critical role in determining its photoconductivity [13] and therefore leads to the change in transmission of terahertz radiation, we investigate the effect of surface treatment on the photoconductivity and photomodulation of electromagnetic radiation with a frequency of $f = 0.13$ THz.

I. Materials and Methods

1.1. Materials

Samples of single-crystalline germanium with a diameter of $d = 30$ mm and a thickness of $h = 0.5$ mm were used. The sample thickness was measured using a Logitech CG10 Contact Gauge (UK). The electrophysical parameters of the studied single-crystalline germanium were measured using a Hall effect measurement system HMS-3000 (France) and are presented in Table 1.

Table 1.

Electrophysical parameters of single-crystalline Ge

Resistivity, ρ, Ohm·cm	60.5
Equilibrium carrier concentration, N_e, cm^{-3}	$3.54 \cdot 10^{13}$
Mobility, μ, $cm^2/V \cdot s$	$2.91 \cdot 10^3$
Conductivity type	*n*

1.2. Methods

1.2.1. Chemical and ionic etching

The working surfaces of the Ge samples were mechanically ground and polished. Chemical etching of the samples was carried out in a solution of the following composition: 95 cm^3 of 1%- KOH and 75 cm^3 of 60%-H_2O_2 with pH = 7–8. The etching process was controlled by the change in thickness and mass of the plate depending on the etching time. The rate of chemical etching of the mechanically treated Ge sample was measured. The rate of the etching process was determined as follows. A strip of PP-383 photoresist was applied to the Ge sample in the middle. The width of the strip was 4 mm. The photoresist was cured for 45 minutes at a temperature of 120˚C. Before the photoresist deposition, the surface of Ge sample was degreased with acetone. Then the sample was subjected to one-sided 1-25 min etching. After the etching completion the photoresist was removed with a concentrated acetone solution and, using the "Dektak A" profilometer, the change in surface irregularities at the interface between the photoresist-protected surface and the etched surface was determined (Fig. 1). The measured etching rate was 70 nm/min.

The surface of Ge samples was also treated by Argon ion etching for 15 min. Ion etching was performed on a Torr International Inc vacuum deposition system.

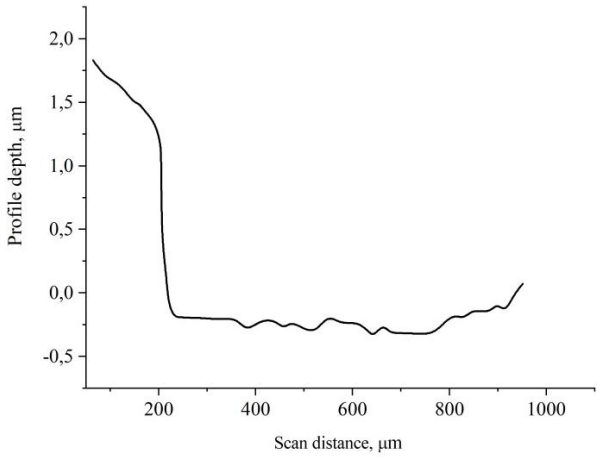

Fig. 1. Change in the surface thickness of a germanium sample at the interface between the surface protected by photoresist and the etched surface. Chemical etching time was 25 min.

1.2.2. Photoconductivity

The photoconductivity of all samples, both mechanically treated and chemically and ion etched, was measured using the Autolab impedance spectrometer (Metrohm Autolab B.V., Netherland) at room temperature. The measurement was performed in the frequency range of 10^{-2} to 10^6 Hz, the signal amplitude was 5 mV. 99 points were set for measurement. Contacts on the surface of the material were deposited in the form of rectangles. The samples were illuminated with a laser light with wavelength of λ=660 nm and power of 32 mW (the beam diameter was 2 mm) without and with the use of neutral filters with optical density: 0.3, 0.64, 1, and in the dark.

1.2.3. Photomodulation

To study the photomodulation of THz radiation, a measuring set-up was proposed, shown in Fig. 2.

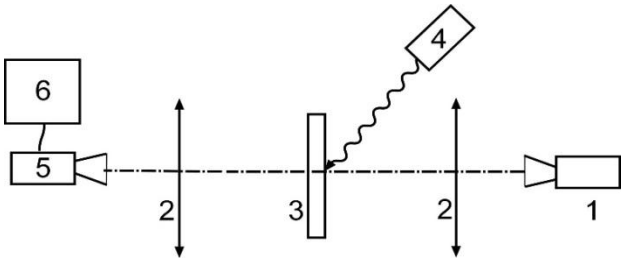

Fig. 2. Set-up for studying photomodulation of THz radiation at a frequency of f=0.13 THz. 1 – transmitter with a horn antenna, 2 – Teflon lenses, 3 – photoconductive material, 4 – SOLIS-565D - High-Power LED (Thorlabs, USA). 5 – receiver with a horn antenna, 6 – Tektronix TDS 3052 oscilloscope.

The emitter (transmitter) of THz radiation operated at a frequency of $f = 0.13$ THz. The transmitter was built on a Si two-span avalanche diode, which was mounted in the generator chamber. The transmitter power level was not less than 10 mW. The active element – a diode –was installed in a generator chamber designed for operation in the THz frequency range. The chamber contains waveguide elements for matching the impedance of the active element and its power supply from a DC source.

The chamber is mechanically fastened to a waveguide flange according to the UG-387/UM standard, which has a waveguide channel WR-07 (1.65x0.83) mm, and positioned on the front panel of the unit. The horn antenna, mechanically fastened to the output flange of the transmitter, forms a directivity diagram and the transmitter signal is radiated. The width of the directivity diagrams of the horns at the half-power level was no more than 10°, and the gain was no less than 25 dB.

Receiver was consisted of a detector, a video signal amplifier and a horn antenna. The useful signal received by the horn antenna, through an intermediate input flange that met the UG-387/UM standard and had a WR-07 (1.65x0.83) mm waveguide channel, entered the detector chamber and was detected, further was amplified and transmitted for indication. The detector was built on a GaAs Schottky diode with a low level of intrinsic noise, which was mounted in a detector waveguide chamber. It provided matching of the diode impedance with the waveguide in the operating frequency range and output of the signal. A video signal amplifier was connected to the output detector to provide a dynamic range of at least 20 dB and an output signal level of at least 100 mV. The output impedance of the video signal amplifier was 1 kOhm.

Illumination with a Solis – 565 D lamp led to photogeneration of carriers. The maximum lamp emission was at a wavelength of λ=565 nm. The lamp radiation power varied in the range from 0.05 W/cm^2 to 0.67 W/cm^2. The lamp flux was modulated in the form of rectangular light pulses with a duration of 1 ms and an interval between pulses of 360 ms (see Fig.3). This made it possible to exclude the influence of thermal generation of charge carriers.

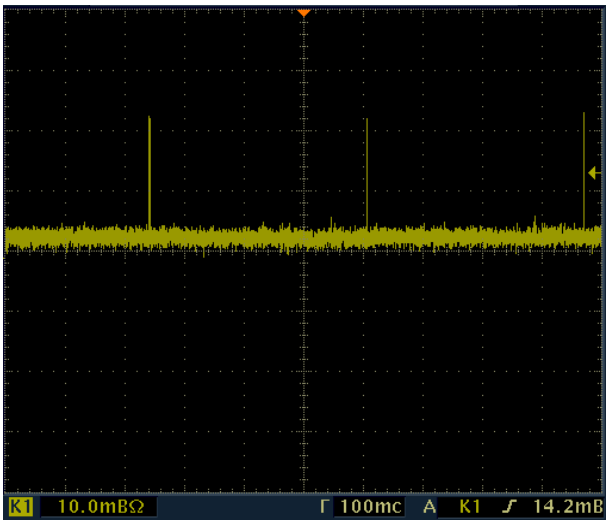

Fig. 3. Modulation of light emission of the Solis– 565 D lamp.

Measurement of the change in the electromagnetic radiation transmission at a frequency of $f = 0.13$ THz by Ge samples illuminated at different power densities (modulation of THz radiation) was carried out according to the following scheme.

Using an oscilloscope we measured:

- the signal on the switched-on THz radiation receiver without electromagnetic radiation (zero level);
- the signal on the receiver when electromagnetic radiation with a frequency of $f = 0.13$ THz is switched on and passed through the air (U_a);
- the signal on the receiver when electromagnetic radiation with a frequency of $f = 0.13$ THz is switched on and passed through the Ge sample (U_s);
- the signal on the receiver when electromagnetic radiation with a frequency of $f = 0.13$ THz is switched on and passed through the illuminated by pulsed optical radiation Ge sample.

The initial transmission of the sample was calculated from the expression $T = U_s/U_a$. The final step is to calculate the transmission for all points of the recorded signal and construct the graphs $T = f(P_i)$, where P_i is the power density of the optical radiation incident on the Ge sample.

II. Results and discussion

2.1. Photoconductivity

Both mechanically treated samples and samples subjected (after mechanical polishing) to ion etching under illumination with maximum power did not reveal any changes in conductivity. The change in conductivity of the chemically etched Ge sample under illumination is presented in Fig. 4a in the form of frequency dependences of the real Re $Z(f)$ (Fig. 4a) part of the impedance, the relative change of photoconductivity (Fig. 4b), and also Nyquist diagrams (Fig. 4c).

As expected, at low frequencies <10^3 Hz (Fig. 4a) the presence of delocalized charge carriers in Ge is observed, which is confirmed by the frequency independence of the material conductivity. With increasing frequency, the conductivity increases, since at higher frequencies (around 10^4 Hz) the contribution to the conductivity is made by the transitions of charge carriers through localized states near the Fermi level [14]. Moreover, a more rapid increase in conductivity at frequencies above 10^4 Hz is observed during measurements in the dark, because of stimulation by illumination, which makes a greater contribution to conductivity, compared to jumps, does not occur, which is obvious from the curves 2-5, Fig. 4a. The results of the studies, presented in Fig. 4, indicate a significant photoconductive response even when using filters that attenuate the illumination power. The relative change of photoconductivity is calculated by the formula:

$$\delta \mathrm{Re}G(f) = \frac{\mathrm{Re}G_i(f) - \mathrm{Re}G_0(f)}{\mathrm{Re}G_0(f)}, \qquad (1)$$

where $\mathrm{Re}G_0(f)$, $\mathrm{Re}G_i(f)$ are the real parts of the conductivity, calculated from the real part of complex impedance, build during measurement in the dark and under laser irradiation, respectively, and are presented in Fig. 4b. As it was expected: with a decrease in optical density of the filters (with an increase in power density of illumination), the relative change of conductivity increases threefold. Its highest value, obtained during measurement without filters, is approximately 5.5. A laser with a wavelength of $\lambda = 660$ nm has a photon energy of ≈ 1.88 eV, which significantly exceeds the bandgap of Ge $E_g \approx 0.66$ eV. Thus, a significant

photoconductive response in germanium occurs mainly due to the generation of a significant number of charge carriers and their high mobility.

When the samples are illuminated, there is a slight decrease in $\delta \mathrm{Re}Z(f)$ at high frequencies, caused by the contribution of jumping conductivity (curves 3, 4, 5) and with the dominance of barrier and polarization processes. The Nyquist diagram (Fig. 4c) on the complex plane along the coordinate axes represents the real Re $Z(f)$ and imaginary Im $Z(f)$ parts of the impedance hodograph. The shape of the impedance hodographs corresponds to the above conclusions and indicates an increase in the conductivity of the material with an increase in the illumination power. Taking into account the nature of the material, as well as the shape of the hodographs, it is obvious that to describe the current flow processes, it is necessary to use the Voight model [15], consisting of two $R||C$ sub circuit. Each of them models a finite conductivity with a corresponding time constant.

2.2. THz radiation photomodulation.

The transmission of THz radiation at a frequency of $f = 0.13$ THz, modulated by light pulses, through a Ge sample that was previously ground, polished, and then chemically etched, is shown in Fig. 5. Fig. 5 shows that when the sample is illuminated with radiation of $P = 0.33$ W/cm^2, the transmission of THz radiation by a chemically etched Ge sample decreases to nearly zero. It is also seen that the modulation time of the THz wave is approximately 2 ms. This time consists of the time of direct modulation of the terahertz wave ~1 ms and the time of return of the sample to the initial (before illumination) state (also approximately 1 ms).

In addition, we also studied the effect of the ground and then etched surface of the Ge sample on the photomodulation of THz radiation with a frequency of $f = 0.13$ THz. Photomodulation of THz radiation with a frequency of $f = 0.13$ THz when it falls on a sample surface is shown in Fig. 6.

It can be seen that the modulation of terahertz radiation is slightly weaker, but at the same time the modulation switching time changes. The efficiency of a terahertz modulator is characterized by the modulation depth MF, which is defined as [16]:

$$MF=(T_0-T_i)/T_0, \qquad (2)$$

where T_0 is the transmittance of THz radiation without optical illumination, T_i is the transmittance at different intensities of optical illumination.

In the case of a chemically etched Ge sample with a ground and polished surface (Fig. 5, 6), the modulation

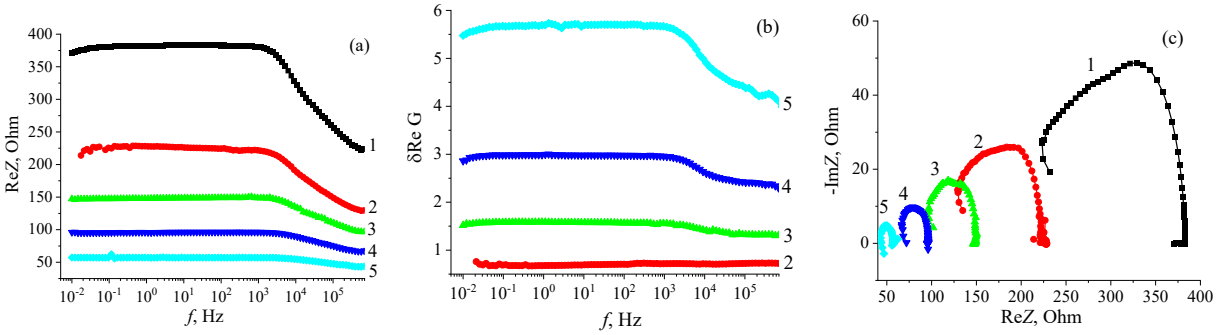

Fig. 4. Frequency dependence of the real part ReZ of complex impedance for (a) a chemically etched Ge sample, relative change of photoconductivity (b), and Nyquist diagram (c), build in the dark (1) and under illumination (λ=660 nm, 32 mW) using neutral filters with optical density: 1(2), 0.64(3), 0.3(4), and without (5) filter.

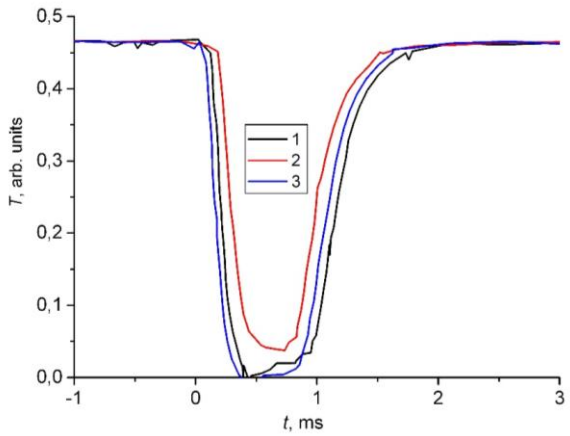

Fig. 5. Transmission of THz radiation with a frequency of $f = 0.13$ THz by a Ge sample that was previously ground, polished, and then chemically etched at different illumination power densities
(1 – $P = 0.12$ W/cm^2, 2 – $P = 0.33$ W/cm^2,
3 – $P = 0.67$ W/cm^2).

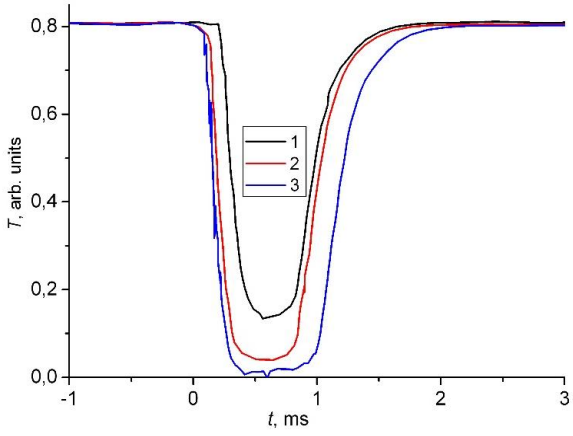

Fig. 6. Transmission of THz radiation with a frequency of $f = 0.13$ THz when it falls on the ground and etched surface of the Ge sample at different illumination power densities
(1 – $P = 0.12$ W/cm^2, 2 – $P = 0.33$ W/cm^2,
3 – $P = 0.67$ W/cm^2).

depth approached 100% for two power densities, $P = 0.33$ W/cm^2 and $P = 0.67$ W/cm^2. For a chemically etched Ge sample with only a ground surface (Fig. 6), the modulation depth was also close to 100%, but only at $P = 0.67$ W/cm^2. The obtained results exceed the data of optical modulation of THz waves at $f = 0.34$ THz for both single-crystalline Ge and modified with gold nanorods [17].

Conclusions

Chemical etching of the single-crystalline Ge surface in a solution consisting of 95 cm³ of 1%-KOH and 75 cm³ of 60%-H_2O_2 with a pH of 7–8 induces a pronounced photoconductive response and enables effective photomodulation of THz radiation by the sample, in contrast to polishing, grinding, or Ar ion etching. Chemical etching of the Ge surface significantly enhances the photogeneration of charge carriers, resulting in a nonlinear increase in photoconductivity by approximately 5.5 times when illuminated with radiation at a wavelength of $\lambda = 660$ nm and a power of 32 mW (beam diameter of 2 mm). This treatment allows achieving an almost 100% modulation depth of THz radiation at a frequency of $f = 0.13$ THz, as experimentally demonstrated with the developed setup. To optimize the parameters of optically controlled THz photomodulators based on single-crystalline Ge, further studies on the influence of sample thickness and the use of alternative chemical etchants are required.

Acknowledgment:

This work was supported by the National Research Foundation of Ukraine (project #2021.01/0410).

Balaban O. – PhD, assoc. Prof., Assoc. prof. of the Department of Applied Physics and Nanomaterials Science;
Bukliv R. – PhD, assoc. prof., Assoc. prof. of the Department of Chemistry and Technology of Inorganic Substances;
Danylov A. – Senior lecturer of the Department of Applied Physics and Nanomaterials Science;
Venhryn B. – PhD, assoc. prof., Assoc. prof. of the Department of Applied Physics and Nanomaterials Science;
Vynnyk D. – junior researcher;
Haiduchok V. – PhD, Head of the Department of Physics of Oxide Crystal Growth, «Electron-Carat» Scientific-Research Company;
Andrushchak A. – DSc, prof., Prof. of the Department of Applied Physics and Nanomaterials Science.

[1] T. M. Narytnyk, A. V. Yermakov, S. O. Bondarchuk, D. S. Valchuk, *Analysis of terahertz technologies and their application for creating innovative developments*, Problems of Telecommunications, 1, 50 (2017); http://nbuv.gov.ua/UJRN/prtel_2017_1_8.
[2] M. Rahm, J.S. Li, W.J. Padilla, *THz wave modulators: A brief review on different modulation techniques*, Journal of Infrared, Millimeter, and Terahertz Waves, 34(1), 1 (2013); https://doi.org/10.1007/s10762-012-9946-2.
[3] S. Guan, J. Cheng, S. Chang, *Recent progress of terahertz spatial light modulators: materials, principles and applications*, Micromachines, 13, 1637 (2022); https://doi.org/10.3390/mi13101637.
[4] P. Gopalan, B. Sensale-Rodriguez, *2D Materials for Terahertz Modulation*, Advanced Optical Materials, 1900550 (2019); https://doi.org/10.1002/adom.201900550.
[5] Z. Wang, J. Qiao, S. Zhao, S. Wang, C. He, X. Tao, S. Wang, *Recent progress in terahertz modulation using photonic structures based on two-dimensional materials,* InfoMat, 3(10), 1110 (2021); https://doi.org/10.1002/inf2.12236.
[6] D. A. B. Miller, *Energy consumption in optical modulators for interconnects,* Optics Express, 20(102), A293 (2012); https://doi.org/10.1364/oe.20.00a293.
[7] Q. Guo, Z. Qin, Z. Wang, Y.-X. Weng, X. Liu, G. Xie, J. Qiu, *Broadly tunable plasmons in doped oxide nanoparticles for ultrafast and broadband mid-infrared all-optical switching*, ACS Nano, 12 (12), 12770 (2018); https://doi.org/10.1021/acsnano.8b07866.
[8] M. Ono, M. Hata, M. Tsunekawa, K. Nozaki, H. Sumikura, H. Chiba, M. Notomi, *Ultrafast and energy-efficient all-optical switching with graphene-loaded deep-subwavelength plasmonic waveguides*, Nat Photonics, 14 (1), 37 (2020); https://doi.org/10.1038/s41566-019-0547-7.
[9] J. Sobolewski, Y. Yashchyshyn, D. Vynnyk, V. Haiduchok, N. Andrushchuk, *Investigation of optically controlled millimeter wave coplanar waveguide photoconductive device*, Acta Physica Polonica A, 141 (4), 420 (2022); https://doi.org/10.12693/APhysPolA.141.420.
[10] N. Andrushchak, D. Vynnyk, M. Melnyk, P. Bajurko, J. Sobolewski, V. Haiduchok, D. Kushnir, A. Andrushchak, Y. Yashchyshyn, *Impact of optical illumination on transmission of subterahertz electromagnetic waves by $Bi_{12}GeO_{20}$ crystals*, Acta Physica Polonica A, 141 (4), 415 (2022); https://doi.org/10.12693/aphyspola.141.415.
[11] A. Kannegulla, Md. I. B. Shams, L. Liu, L.-J. Cheng, *Photo-induced spatial modulation of THz waves: opportunities and limitations,* Optics Express, 23 (25), 32098 (2015); https://doi.org/10.1364/OE.23.032098.
[12] Y. Li, D. Zhang, Y. Liao, Q. Wen, Z. Zhong, T.Wen, *Interface engineered germanium for infrared THz modulation*, Optical Materials, 111, 110659 (2021), https://doi.org/10.1016/j.optmat.2020.110659.
[13] G.P. Peka, B.I. Strikha, Surface and contact phenomena in semiconductors (Lybid, Kyiv, 1992).

[14] M. Pollak, T.H. Geballe, *Low-frequency conductivity due to hopping processes in silicon,* Phys. Rev, 122(6), 1742 (1961); https://doi.org/10.1103/PhysRev.122.1742.
[15] J.R. McDonald, *Impedance spectroscopy and its use in analyzing the steady-state response of solid and liquid electrolytes*, Journal of Electroanalytical Chemistry and Interfacial Electrochemistry, 223(1-2), 25 (1987); https://doi.org/10.1016/0022-0728(87)85249-X.
[16] I.R. Hooper, N.E. Grant, L.E. Barr, S. M. Hornett, J. D. Murphy, E. Hendry, *High efficiency photomodulators for millimeter wave and THz radiation*. Scientific Reports, 9, 18304 (2019); https://doi.org/10.1038/s41598-019-54011-6.
[17] Y. Li, D. Zhang, Y. Liao, Q. Wen, Z. Zhong, T. Wen, *Interface engineered germanium for infrared THz modulation*, 111, 110659 (2021); https://doi.org/10.1016/j.optmat.2020.110659.

О. Балабан[1], Р. Буклів[1], А. Данилов[1], Б. Венгрин[1], Д. Винник[1], В. Гайдучок[2], А. Андрущак[1]

Вплив обробки поверхні монокристалічного Ge на його фотопровідність і фотомодуляцію випромінювання частотою 0,13 ТГц

[1]*Національний університет «Львівська політехніка», Львів, Україна, bohdan.y.venhryn@lpnu.ua*
[2]*Науково-виробниче підприємство «Електрон-Карат», Львів, Україна*

Досліджено вплив механічної обробки, іонного та хімічного травлення поверхні монокристалічного германію на його фотопровідність та можливість фотомодуляції в терагерцовій ділянці спектру. Визначено відносні зміни електропровідності матеріалу під впливом освітлення лазерним випроміненням з довжиною хвилі 660 нм при різних потужностях опромінення. Створено установку для дослідження фотомодуляційних властивостей германію на частоті 0,13ТГц і виявлено різке збільшення поглинання такого електромагнітного випромінювання навіть при малих потужностях освітлення.

Ключові слова: напівпровідники, монокристалічний германій, хімічне травлення поверхні, фотопровідність, терагерцове випромінювання, фотомодуляція.